Marine Biology (2025) 172:114
https://doi.org/10.1007/s00227-025-04648-x

ORIGINAL PAPER

Reproductive biology of two hydrothermal vent Cocculinidae species (Mollusca: Gastropoda) from the Arctic and Southern Ocean

Christopher MacNeil[1] · **Maria Baker**[1] · **Jon Copley**[1] · **Paul Tyler**[1] · **Ana Hilario**[2] · **Eva Ramirez-Llodra**[3]

Received: 26 June 2024 / Accepted: 29 April 2025 / Published online: 13 June 2025

Abstract

The ecology of hydrothermal vents in polar oceans is less known than other regions, as a consequence of the logistical challenges of deep-sea fieldwork at high latitudes, and particularly under permanent ice cover in the Arctic. This paper describes the reproductive biology of the first two cocculinid gastropods sampled from hydrothermal vents: *Cocculina enigmadonta* from Kemp Caldera, in the Southern Ocean, and *Cocculina aurora* (Chen et al., Royal Soc Open Sci, https://doi.org/10.1098/rsos.220885, 2022) from the Aurora Vent Field, Gakkel Ridge, in the Central Arctic Ocean. Histological analysis was used to describe oogenesis, size at first reproduction and fecundity, whilst individual size-frequency distributions from morphometric measurements were produced to investigate demographic population structure. Both species exhibited similar gametogenic patterns with all but three individuals possessing all oocyte developmental stages. *Cocculina enigmadonta* and *C. aurora* had similar reproductive strategies, exhibiting low fecundities. For *C. enigmadonta* the mean fecundity was 16.1 ± 9.3 mature oocytes and for *C. aurora* 4.1 ± 2.4 mature oocytes. Gametogenic maturity, mean oocyte diameter and instantaneous fecundity were statistically significantly different between species. Overall, both species presented asynchronous reproduction, quasi-continuous gametogenesis and discontinuous recruitment. Importantly, our results provide the first account of the reproductive biology of cocculinid species from hydrothermal vents and discuss their adaptive life-history traits to inhabiting unstable vent environments.

Keywords *Cocculina* · Deep ocean · Fecundity · Oogenesis · Recruitment

Introduction

The deep ocean is a vast biome without sunlight which includes chemosynthetic habitats such as hydrothermal vents and cold seeps (Ramirez-Llodra et al. 2010). These habitats host high in situ microbial primary productivity via chemosynthesis (Tyler and Young 1999; Van Dover 2000), which in turn supports a high faunal biomass compared with other deep-sea environments, and a high level of taxonomic endemism (Kelly and Metaxas 2007; Chen and Linse 2020; Yahagi et al. 2020). Hydrothermal vents are dynamic chemosynthetic environments, with temperature and chemical gradients that fluctuate over short time-scales and spatial-scales (Bayer et al. 2011). Individual vent fields represent insular habitats, separated by tens to hundreds of kilometres (Matabos and Thiebaut 2010; Bayer et al. 2011; Marticorena et al. 2020), that are ephemeral over timescales of decades to millennia in hydrothermal activity that supports local chemosynthesis (Kelly and Metaxas 2007).

The ability of a population to adapt and recover from natural and anthropogenic disturbances is tightly linked to reproductive patterns including age at maturity, gametogenesis, fecundity, and oocyte size (Olabarria and Ramirez-Llodra 2004; Marticorena et al. 2020). Although research of the life history of organisms inhabiting chemosynthetic environments is improving, knowledge of the ecology of chemosynthetic environments in high latitudes is constrained by logistical challenges of conducting deep-sea fieldwork in

Communicated by J. Grassle.

✉ Maria Baker
mcb3@soton.ac.uk

Christopher MacNeil
christopher@macneil.me.uk

[1] University of Southampton, Southampton, UK

[2] Centre for Environmental and Marine Studies, Department of Biology, University of Aveiro, Aveiro, Portugal

[3] REV Ocean, Lysaker, Norway

polar regions. Additionally, sampling restraints often limit studies of reproductive biology and gametogenesis to one-time analyses, with minimal spatio-temporal studies (Matabos and Thiebaut 2010).

Gastropods are a widespread taxonomic group at hydrothermal vents. The majority of vent gastropods studied to date have vitellogenic mechanisms and reproductive patterns that are phylogenetically constrained to internal fertilisation and lecithotrophic development (Lutz et al. 1984; Kelly and Metaxas 2007; Tyler et al. 2008). Other factors including, oocyte size and fecundity can be influenced by environmental conditions (Ramirez-Llodra 2002). Larval development in gastropods can be inferred from oocyte size and fecundity. Most vent gastropod species exhibit quasi-continuous egg production and reproduce continuously, which may be attributed to the constant supply of energy from chemosynthesis (Rokop 1977; Bayer et al. 2011; Marticorena et al. 2020). In general, lecithotrophic species produce eggs that are greater than 200 µm in small quantities and planktotrophic species produce eggs that are smaller than 200 µm in high quantities (Jaeckle 1995; Levin and Bridges 1995; Marticorena et al. 2020). It is possible to derive important information about larval dispersal and development from indirect methods (Tyler et al. 2008), for example, using the morphology of the protoconch in gastropods to determine information relating to larval development (Lutz 1988; Gustafson et al. 1991; Tyler et al. 2008; Matabos and Thiebaut 2010). The shell of gastropods has two development stages, corresponding to the formation of the embryonic shell (protoconch I) and larval shell (protoconch II) (Vrijenhoek 1997; Nützel et al. 2006; Hoffman et al. 2020). Planktotrophic gastropods possess both protoconch development stages, with a small protoconch I and a large protoconch II. Conversely, lecithotrophic species possess a bulbous/large protoconch I and a small or absent protoconch II (Vrijenhoek 1997; Hoffman et al. 2020).

The family Cocculinidae belongs in the subclass Neomphaliones, order Cocculinida. Individuals are hermaphroditic, roughly symmetrical gastropods and are usually smaller than 1 cm in length (Bouchet et al. 2017; Chen and Linse 2020). The genus *Cocculina* is represented by at least 20 species mainly associated with sunken organic wood falls. However, two further species have been reported in association with whale falls, *Cocculina craigsmithi* (McLean 1992) and *Cocculina delphinicula* (Zhang and Zhang 2018), and two from hydrothermal vents, *Coccculina enigmadonta* (Chen and Linse 2020) and *Cocculina aurora* (Chen et al. 2022). Cocculinids possess a protoconch that is bulbous and lacks a protoconch-II (Young et al. 2013), and in addition the protoconch is symmetrical (Haszprunar 1988) and reticulately sculptured (Marshall 1985). This structure in cocculinids is indicative of lecithotrophic larval development (Marshall 1985; Haszprunar 1988; Vrijenhoek 1997; Young et al. 2013; Hoffman et al. 2020; Chen et al. 2022).

Cocculinids inhabiting hydrothermal vents (*Cocculina enigmadonta*) were reported from Kemp Caldera, Antarctica (59°42'S, 28°20'W) (Chen and Linse 2020). Kemp Caldera ranges in depth from 900 to 1600 m from sill to base and is dominated by chemosymbiotic vesicomyid clams and cocculinid limpets (Linse et al. 2019; Chen and Linse 2020). The caldera consists of a central resurgent cone surrounded by diffuse-flow vents and white-smokers (Roterman et al. 2016; Chen and Linse 2020). A natural whale fall was discovered at a depth of 1444 m in close proximity (~ 250 m) to the active hydrothermal vent area (Amon et al. 2013). Only two species were found to inhabit both the vent and the whale fall, namely *C. enigmadonta* and the vetigastropod limpet *Lepetodrilus concentricus.* Chen and Linse (2020) completed an extensive study on *C. enigmadonta* morphology and evolutionary history, which found evidence for the transition of *C. enigmadonta* from organic falls to hydrothermal vent environments.

During investigations of the Aurora Vent Field (AVF, 82.5 N) (Fig. 1a, b) on the Gakkel Ridge, Central Arctic Ocean (Bünz et al. 2021; German et al. 2022; Ramirez-Llodra et al. 2022) a new species of cocculinid, *Cocculina aurora* (Chen et al. 2022) was found and sampled from active hydrothermal vents. The Gakkel Ridge is 1800 km in length and stretches across the Arctic Ocean and Eurasian Basin (Michael et al. 2003) and it shows evidence of more than nine discrete hydrothermal vent fields (Edmonds et al. 2003). The AVF is situated towards the Southwest of the Gakkel Ridge (Michael et al. 2003) and sits on the flank of the Aurora mound. It was first located during the Arctic Mid-Ocean Ridge Expedition (AMORE) 2001 (Edmonds et al. 2003), via water chemistry signals from the rising plume and the collection of hydrothermal vent chimney pieces using a dredge. The black smokers of the AVF (Fig. 2a, b), however, were not located until 2014 during the Polarstern PS86 Aurora expedition, which provided the first visual evidence of the active AVF (Boetius 2015; German et al. 2022). During the HACON21 cruise on board RV *Kronprins Haakon*, the AVF was surveyed and sampled with a Remote Operated Vehicle (ROV), conducting the first ROV dives on a deep vent field under permanent ice-cover (Ramirez-Llodra et al. 2022).

Currently, *C. enigmadonta* and *C. aurora* are the only cocculinid species sampled from hydrothermal vents. The main objectives of this study were to investigate and compare the reproductive biology and population structure of *C. enigmadonta* and *C. aurora* sampled from hydrothermal vents in the Southern Ocean and Arctic Ocean respectively. This study examines oogenesis, oocyte size, minimum size of maturity and estimates fecundity to characterise

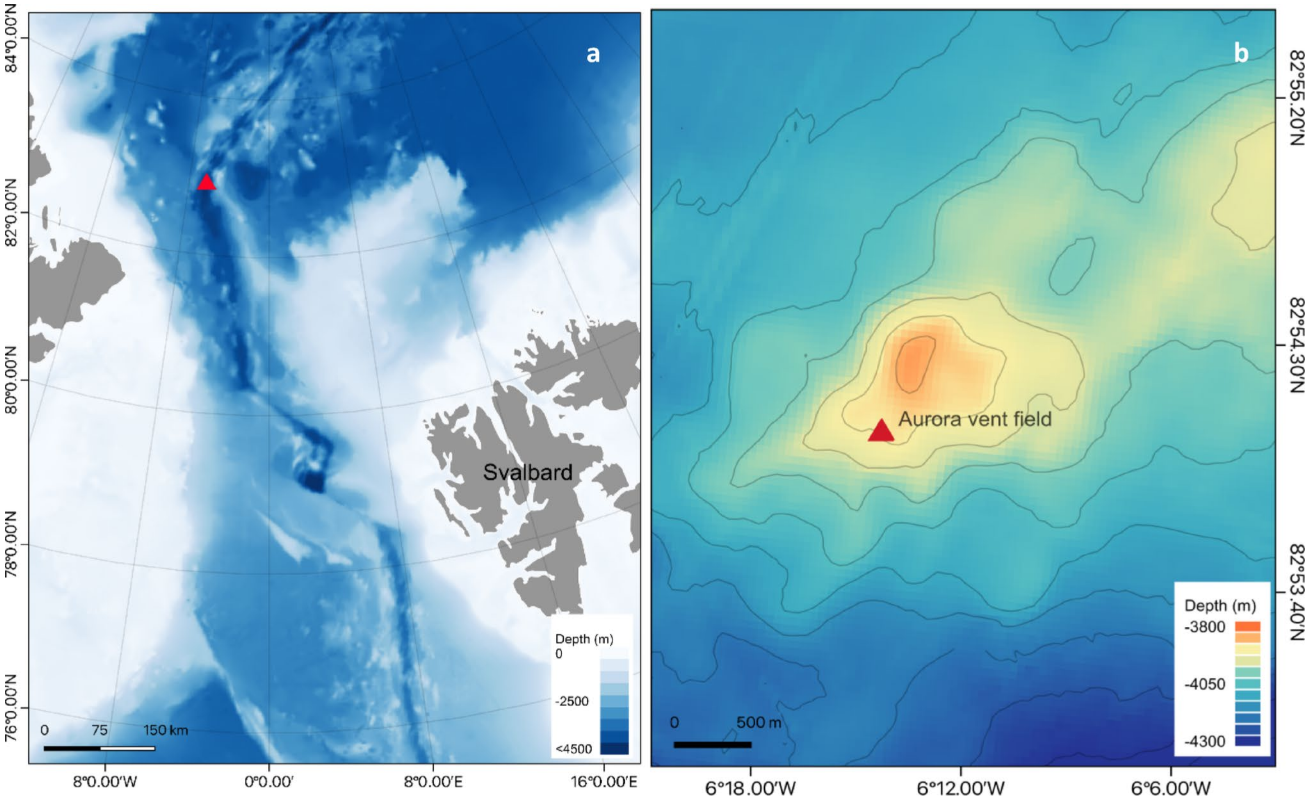

Fig. 1 (**a**) Geographic location of the Aurora Vent Field on the Gakkel Ridge. (**b**) Sampling area of *C. aurora.* Red triangle: Aurora Vent Field. (**a–b**) Produced from the HACON21 expedition and used with permission

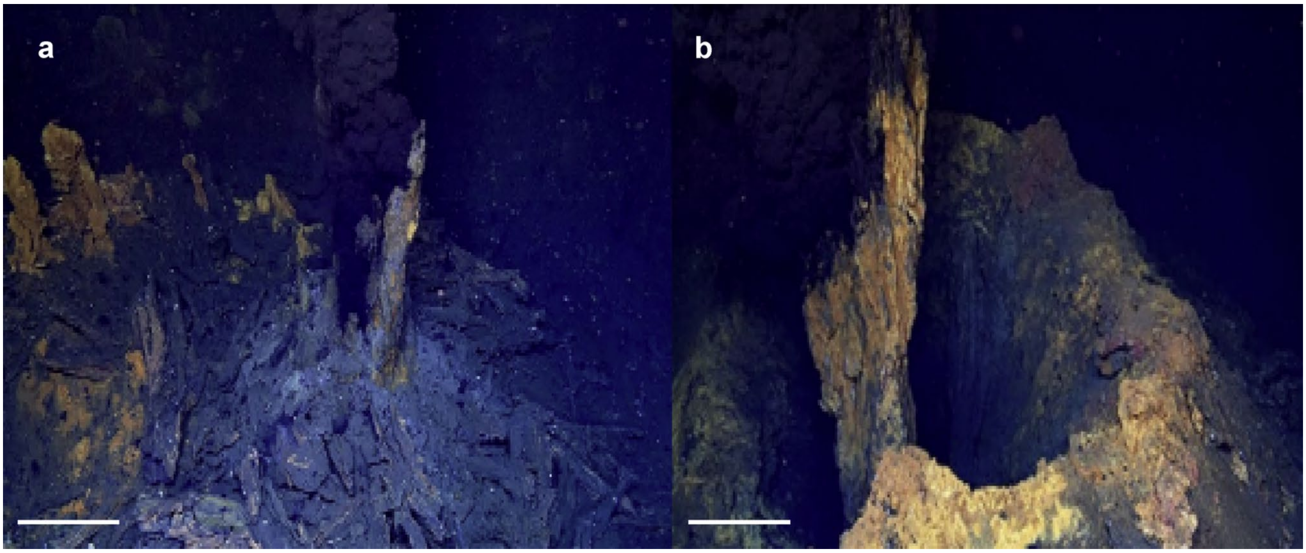

Fig. 2 Black smoker hydrothermal vents in the Aurora Vent Field. (**a**) Ganymede vent and (**b**) Hans Tore vent. The white scale bar is approximately 50 cm

reproductive patterns and infer reproductive adaptations for inhabiting hydrothermal vent environments. Further, the population structure was compared between taxa and spatial variability was assessed between *C. aurora* populations sampled from two hydrothermal vents 6 m apart in the AVF.

Materials and methods

Field sampling

Cocculina enigmadonta specimens were sampled from

Kemp Caldera, Southern Ocean (59°42′S, 28°20′W) in 2010 during RRS *James Cook* Expedition JC42. The ROV *Isis* was used to collect samples from hydrothermal vents at depths from 1375 to 1487 m. Specimens of the newly identified species *C. aurora* were collected during the HACON21 expedition on the RV *Kronprins Haakon* in October 2021. Individuals were sampled using the ROV *Aurora* from the AVF (82°53’N, 6°15’W). Samples were collected from two vents, the Ganymede vent at a depth of 3884 m and the Hans Tore vent, ~ 6 m north of the Ganymede vent, at a depth of 3883 m (Fig. 2a, b). Both *C. enigmadonta* and *C. aurora*, specimens were sampled using a manipulator arm and suction sampler. *Cocculina enigmadonta* individuals from Kemp Caldera were preserved in 96% ethanol. *Cocculina aurora* specimens, attached to a large piece of old hydrothermal vent chimney, were fixed in 4% formaldehyde for 48 h before being transferred to 70% ethanol. Some individuals were frozen for taxonomic and molecular studies.

Population structure

In the laboratory, the 153 individuals of *C. enigmadonta* and 148 individuals of *C. aurora* were labelled corresponding to species and sampling sites. Each individual was photographed using a dissecting microscope with a mounted camera and the Olympus cellSens Dimension software was used to measure all individuals. For *C. enigmadonta*, body length and width were measured, as the soft bodies of most specimens were already separated from the shell (Fig. 3a). Shell length and width were measured for *C. aurora* (Fig. 3b). 0.5 mm was chosen as an appropriate size-class interval for both *C. enigmadonta* and *C. aurora* for this study (sensu Kelly and Metaxas 2008). Length-frequency histograms were produced to analyse the distribution of cocculinid samples at the time of sampling as temporal analysis was not available. All statistical analysis was completed using SPSS, unless otherwise stated. A Kolmogorov-Smirnov test was used to compare the length-frequency distributions against a normal distribution to evaluate whether the structure of the population matches a typical normal distribution. When the length-frequency distributions were found to be significantly different from a normal distribution, and assuming each cohort analysed followed a gaussian distribution, modal decomposition was performed using the R package Mixdist (Macdonald 2018). Bhattacharya’s method (1967) adapted by Paul and Caddy (1985) was first used to estimate mean and standard deviations. At least 100–300 specimens are required for a good representation of the population, thus modal decomposition analysis could not be completed for *C. aurora* at each vent site as there were fewer than 100 individuals. However, the populations were combined to allow for an appropriate modal decomposition to be conducted. A two-sample Kolmogorov-Smirnov test was used to assess if there was a significant difference between the length-frequency distributions between the two species and between *C. aurora* sampled from the two different black smokers on the AVF.

Reproductive biology

The shells of *C. aurora* individuals were removed from the body using forceps. For histological analysis, eosin was added to the samples of both species prior to processing, to help visualise the organisms during processing. Individuals were dehydrated using a series of graded isopropan-2-ol solutions, cleared in Histoclear, and then embedded in paraffin wax. Individuals were orientated perpendicular to the embedding cassettes with the ventral side of the organism facing downwards. *Cocculina enigmadonta* specimens were sectioned at 7 µm, whilst *C. aurora* individuals were

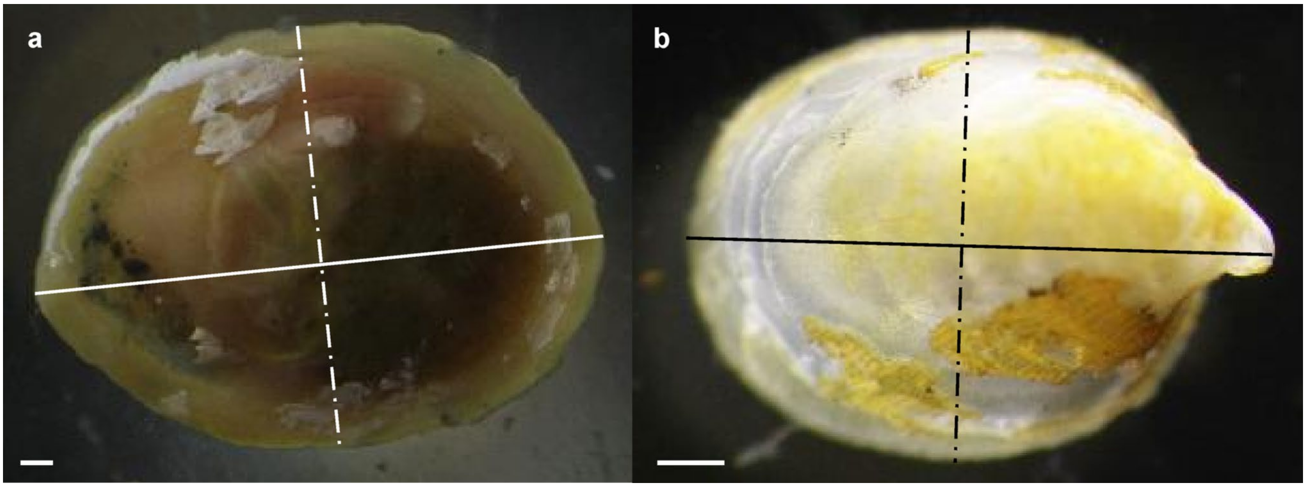

Fig. 3 Morphometric measurements for (**a**) *C. enigmadonta* and (**b**) *C. aurora*. Normal line: body/shell length and dotted line: body/shell width. White scale bar represents 500 µm

sectioned at 5 µm using a rotary microtome, because of their relative sizes. Haematoxylin and eosin were used for biological staining of each specimen and stained sections were preserved in DPX mounting medium. Observations and photographs of histological slides were taken using a Nikon stereomicroscope mounted with a Nikon D5000 Camera.

For gametogenic analysis, ImageJ software (Schneider et al. 2012) was used to count and measure the equivalent circular diameter (ECD) of the oocytes. In both *C. enigmadonta* and *C. aurora*, at least fifty oocytes per individual were counted from four to five serial sections. Fifty oocytes were chosen to maximize individuals available for analysis and to ensure the oocyte sampling size was adequate. ECD was measured for each oocyte and is considered to be ‘the best-fit spherical size of each oocyte’. Although Oocyte Feret Diameter is equivalent to ECD, ECD was considered a more appropriate term (Lau et al. 2018). The oocytes counted and measured were limited to those sectioned directly through the nuclei. Furthermore, photographs of overlaying sections were compared to ensure no oocytes were counted more than once. In total, 72 individuals of *C. enigmadonta* and 58 *C. aurora* individuals (22 from the Ganymede vent and 36 from the Hans Tore vent) were suitable for histological processing. Gametogenic maturity for each specimen was determined as the percentage of mature oocytes of the total number of oocytes measured. Gametogenic maturity and mean oocyte diameter were correlated against length using Spearman’s rank correlation tests and Kruskal-Wallis tests were used to assess if there was a significant difference between species. Oocyte sizes were defined and grouped into size classes of 10 µm to create size-frequency figures. Non-parametric Kruskal-Wallis multi-sample tests were undertaken to identify intra-sample, inter-species, and stage variation in size-frequency distributions. Individuals that caused a significant variation were then identified using a post-hoc Dunn test. Additionally, the mean oocyte diameter of each oocyte development size per individual was compared between species and between the two vent sites for *C. aurora* using a MANOVA Wilk’s Test. No evidence of spermatogenesis was found in *C. enigmadonta*. Different stages of spermatogenesis were found synchronously in many individuals of *C. aurora*, but could not be quantified accurately.

Fecundity in both *C. enigmadonta* and *C. aurora* was determined using serial sections. The median diameter of vitellogenic oocytes was determined by serial sectioning of eight individuals of each species. Sectioning was then completed at the median size, with overlying sections compared to ensure mature oocytes were not counted twice. From this process, instantaneous fecundity was quantified by counting all mature oocytes from the sections. Instantaneous fecundity was correlated against length and Kruskal-Wallis tests were used to assess if instantaneous fecundity was significantly different between species and between vent sites for *C. aurora* populations. Furthermore, the minimum size of reproductive maturity was determined as the smallest size when an individual possessed at least one mature oocyte.

Results

Population structure

The body length of *C. enigmadonta*, ranged between 4.76 and 9.95 mm (Fig. 4a). For *C. aurora*, shell length ranged from 1.36 to 4.77 mm in specimens from the Ganymede vent (Fig. 4b) and 0.85–5.51 mm for specimens from the Hans Tore vent (Fig. 4c). All distributions were statistically significantly different from a normal distribution (Kolomogorov Smirnov tests ($p < 0.05$). All length-frequency distributions were dominated by medium to larger sized individuals; thus, distributions were negatively skewed. All distributions had a dominant peak, which was evident between 8.0 and 8.5 mm for *C. enigmadonta* and between 3.0 and 4.0 mm for *C. aurora*. Modal decomposition with Mixdist exhibited two gaussian components for both species, however further analysis showed neither of the distributions exhibited meaningful cohorts, thus have not been included. There was a significant difference in length between *C. enigmadonta* and *C. aurora* (Two sample Kolmogorov-Sample test, Z = 8.646, $N1 = 153$, $N2 = 148$, $p < 0.05$). In addition, a two sample Kolmogorov-Smirnov test indicated there was no significant difference in shell length between the two *C. aurora* population distributions at Ganymede and Hans Tore vents (Z = 0.909, $N1 = 63$, $N2 = 91$, $p = 0.381$).

Gametogenesis

In both cocculinid species, histology showed that all stages of oogenesis were evident (Table 1; Fig. 5c, f), with oogonia, previtellogenic, vitellogenic and mature oocytes present within individuals. Oogonia are occupied almost entirely by their nucleus and develop in the germinal epithelium, which extends into the ovary. This explains why oogonia were present throughout the entire ovary. In *C. enigmadonta*, the oogonia grow to around 35 µm before becoming previtellogenic oocytes, while oogonia grow to around 20 µm in *C. aurora*. Previtellogenic oocytes are composed of basophilic cytoplasm which stains purple with haematoxylin, with a small cytoplasm/nucleus size ratio. Vitellogenesis starts at an oocyte diameter between 70 and 80 µm for *C. enigmadonta* and a diameter between 40 and 55 µm for *C. aurora*. At the beginning of vitellogenesis, yolk granules become visible towards the periphery of the oocyte. Vitellogenic

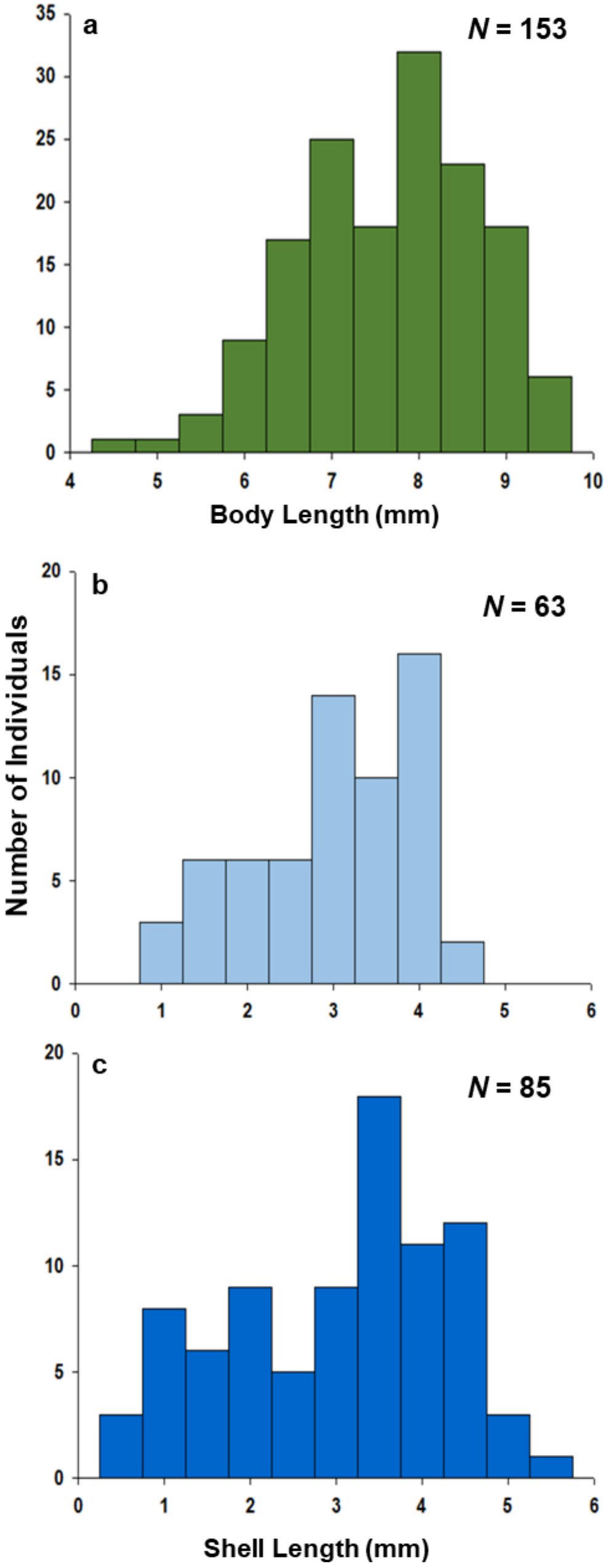

Fig. 4 (**a**) Body length-frequency distributions for *C. enigmadonta*. Shell length-frequencies for *C. aurora* from the (**b**) Ganymede vent and (**c**) Hans Tore vent. *N*: number of individuals measured

oocytes are histologically characterised by a prominent nucleus and acidophilic granular cytoplasm, with large cytoplasm/nucleus size ratio (Fig. 5c, f). Mature oocytes had reached their maximum size and were ready to spawn. In addition, at this stage the nucleolus became barely visible. Mature oocytes diameter were recorded between 131.4 and 185.3 µm in *C. enigmadonta* and between 102.2 and 183.8 µm in *C. aurora* (Table 1).

Significant differences were found in the mean oocyte diameter at each stage of oocyte development between *C. enigmadonta* and *C. aurora* (MANOVA Wilk's, F= 1460.96, $p < 0.001$). However, there was no statistically significant difference between the mean oocyte diameter of the four oocyte development stages among vent sites for *C. aurora* (MANOVA Wilk's, F = 2.215, $p = 0.081$), suggesting a lack of spatial variation in oogenesis among our samples of this species (Fig. 6).

There was no evidence of spermatogenesis in *C. enigmadonta*. Conversely, there was evidence of spermatogenesis in different stages in numerous individuals of *C. aurora* (Fig. 5f), however each stage of spermatogenesis could not be quantified with accuracy.

Oocyte size-frequency distributions

For *C. enigmadonta*, oocyte diameter ranged from 20.9 to 185.3 µm (Table 1). There were two evident peaks, exhibiting a bimodal distribution and suggest periodic asynchronous spawning events. The first peak between 40 and 55 µm was attributed to previtellogenic oocytes and the second peak between 120 and 130 µm corresponded to vitellogenic oocytes (Fig. 7a). Both peaks were produced by a similar percentage of total oocytes. A Kruskal-Wallis multi-sample test showed significant intra-sample variation in oocyte-size frequency for *C. enigmadonta* (H =584.420, df =71, $p < 0.001$). A post hoc Dunn's multi-sample test indicated that around six to eight individuals of *C. enigmadonta* accounted for the significant variation in oocyte-size frequencies. Gametogenic maturity in individuals which possessed mature oocytes ranged from 4.2 to 32.7%, with a mean of 15.7 ± 6.7%, indicating high disparity. Mean oocyte diameter ranged from 45.0 to 110.8 µm across each specimen of *C. enigmadonta* (Fig. 8). No significant correlation was found between body length and mean oocyte diameter (Spearman's rank correlation, $r_s = 0.126$, $R^2 = 0.091$, $N = 72$, $p = 0.291$) or gametogenic maturity (Spearman's rank correlation, $r_s = 0.039$, $R^2 = 0.009$, $N = 72$, $p = 0.746$).

For *C. aurora*, oocyte diameter ranged from 14.1 to 183.8 µm (Table 1). Oocyte-size distributions were determined to have a positively skewed pattern. The *C. aurora* oocyte size-frequency distributions had a clear peak between 20 and 40 µm, attributed to previtellogenic oocytes. This peak

Table 1 Summary of reproductive traits for *C. enigmadonta* and *C. Aurora*. *n*: number, OO: oogonia, PVO: previtellogenic oocytes, VO: vitellogenic oocytes and MO: mature oocytes

Species	*C. enigmadonta*			*C. aurora*					
Vent				Ganymede			Hans Tore		
	Mean (± SD)	Range	*n*	Mean (± SD)	Range	*n*	Mean (± SD)	Range	*n*
OO	32.1 ± 3.2	20.9–36.9	200	18.6 ± 1.5	14.1–21.6	60	18.7 ± 1.5	12.2–22.9	113
PVO	54.1 ± 10.8	34.7–82.9	2802	32.1 ± 6.7	20.0–56.5	969	31.9 ± 6.8	20.0–55.7	1649
VO	118.6 ± 15.7	69.0–149.1	2919	68.9 ± 17.8	39.8–113.7	406	65.8 ± 15.8	39.9–111.1	721
MO	149.0 ± 8.9	131.4–185.3	1113	128.4 ± 14.7	106–178.7	82	129.7 ± 17.9	102.2–183.8	157

made up approximately 60% of oocytes in *C. aurora* specimens. Furthermore, there appeared to be a minor peak at 120–130 µm, which corresponded to mature oocytes. There was significant intra-sample variation in oocyte-size distributions for the specimens from both vent sites (Kruskal-Wallis multi-sample tests: Ganymede: $H = 63.838$, $df = 21$, $p < 0.001$ and Hans Tore: $H = 67.682$, $df = 35$, $p < 0.001$). The intra-sample variation was caused by two to four individuals at each site, as determined by a Post Hoc Dunn's multi-sample test. There was no significant spatial variation in oocyte-size distribution of *C. aurora* between the two sampling locations (Kruskal-Wallis test, $H = 0.03$, $df = 1$, $p = 0.863$). Gametogenic maturity ranged from 1.52 to 13.2%, with a mean gametogenic maturity of 5.7 ± 3.1%. Gametogenic maturity was independent from shell length at both vent sites (Spearman's rank correlation, Ganymede: $rs = 0.289$, $R^2 = 0.122$, $N = 22$, $p = 0.192$ and Hans Tore: $rs = 0.010$, $R^2 = 0.001$, $N = 36$, $p = 0.955$). There was a significant correlation between mean oocyte diameter and shell length of *C. aurora* sampled from the Ganymede vent (Spearman rank correlation, $rs = 0.467$, $R^2 = 0.285$, $N = 22$, $p < 0.05$; Fig. 8). In contrast, individuals sampled from the Hans Tore vent showed no statistically significant correlation between mean oocyte diameter and shell length (Spearman rank correlation, $rs = 0.190$, $R^2 = 0.022$, $N = 36$, $p = 0.267$; Fig. 8). Furthermore, gametogenic maturity and mean oocyte diameter were significantly different between each species (Kruskal-Wallis test, gametogenic maturity: $H = 56.515$, $df = 1$, $p < 0.001$ and mean oocyte diameter: $H = 91.198$, $df = 1$, $p < 0.001$).

Fecundity

From the 72 individuals of *C. enigmadonta* histologically processed, only three did not possess mature oocytes ($SL = 4.76$, 6.41 and 8.96 mm). The smallest-sized individual that possessed mature oocytes measured 5.23 mm, which can therefore be inferred as an estimate of the minimum size for the onset of reproductive development. Instantaneous fecundity was low and showed considerable variation for *C. enigmadonta*, ranging from 3 to 39 mature oocytes with a mean of 16.1 ± 9.3 mature oocytes. Body length and instantaneous fecundity did not exhibit a statistically significant correlation (Spearman rank correlation, $r_s = 0.156$, $R^2 = 0.042$, $N = 72$, $p = 0.189$).

Two individuals of *C. aurora* at the Ganymede vent ($SL = 2.77$ and 3.06 mm) and one individual at the Hans Tore vent ($SL = 4.05$ mm) did not contain mature oocytes. The smallest-sized individual that possessed mature oocytes was 2.70 mm and 1.62 mm at the Ganymede and Hans Tore vent respectively. A Kruskal-Wallis test showed no statistically significant difference in instantaneous fecundity between the two black smoker vent sites in the AVF ($H = 0.939$, $df = 1$, $p = 0.333$). Thus, there was no apparent spatial variation in relation to instantaneous fecundity. Instantaneous fecundity was low and ranged from 1 to 12 mature oocytes, with a mean of 4.1 ± 2.4 mature oocytes. Shell length and instantaneous fecundity did not have a statistically significant correlation at both vent sites (Spearman rank correlation: Ganymede: $r_s = 0.291$, $R^2 = 0.130$, $N = 22$, $p = 0.189$ and Hans Tore: $r_s = 0.003$, $R^2 = 0.0006$, $N = 36$, $p = 0.986$). However, instantaneous fecundity did show inter-species variation and was significantly different between *C. enigmadonta* and *C. aurora* (Kruskal-Wallis test, $H = 65.390$ $df = 1$, $p < 0.001$).

Discussion

Recruitment and population structure

In *C. enigmadonta* and *C. aurora*, length-frequency distributions were negatively skewed, with distributions dominated by bigger organisms, suggesting a high juvenile growth rate and/or high juvenile mortality (Bayer et al. 2011). Conversely, McHugh (1989) suggested the possibility of juvenile negative sampling bias, which may occur if adults and juveniles are spatially segregated. There were distinct peaks in the length-frequency distributions for both species and at each vent site for *C. aurora.* From statistical analysis there was no significant difference between the length frequencies of *C. aurora* sampled from each vent site. Although variation can occur on small scales, the Hans Tore vent and Ganymede vent are only separated by 6 m, thus it is likely individuals of *C. aurora* at the different vents would possess

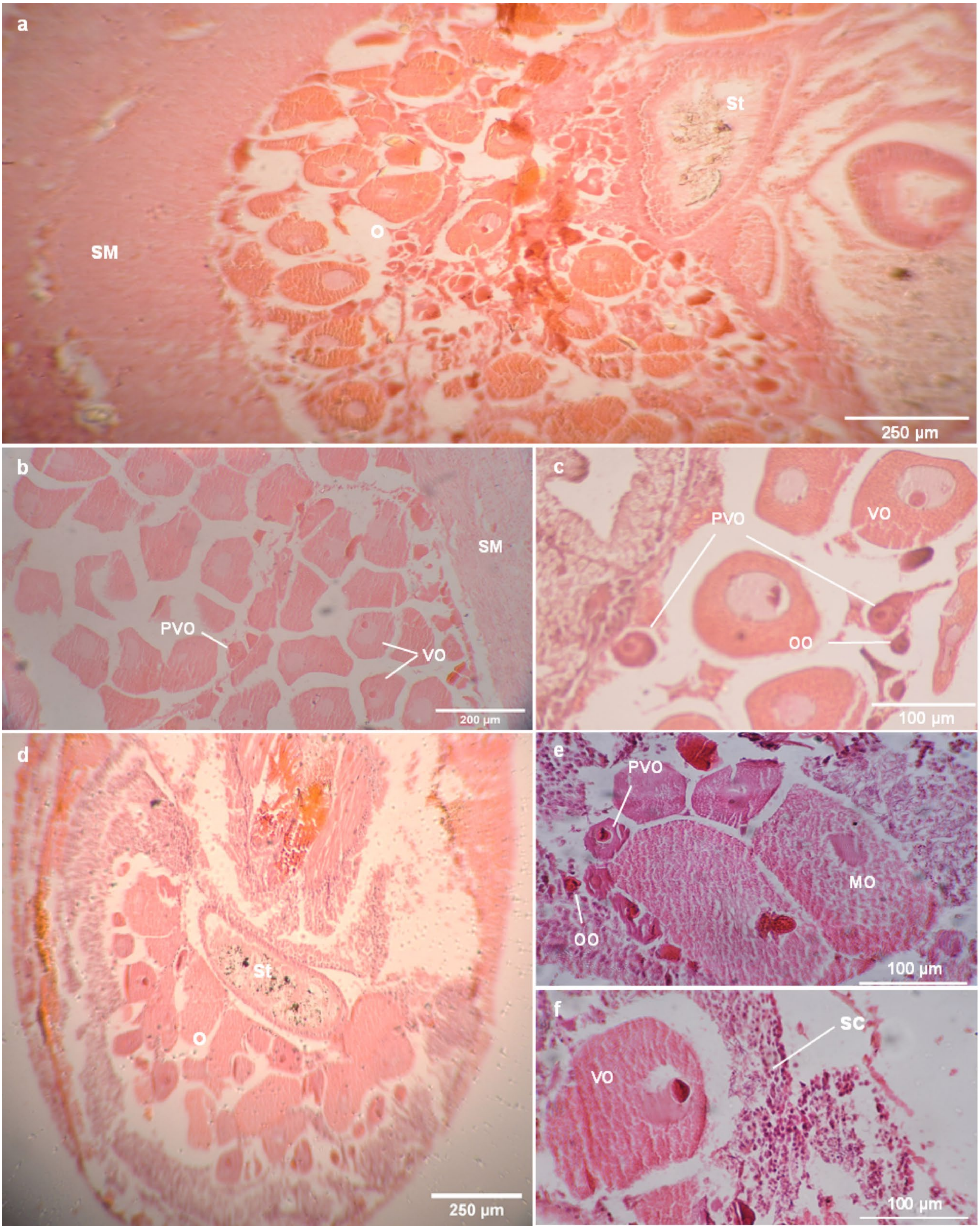

Fig. 5 Ovarian structure of *C. enigmadonta* and *C. aurora*. (**a**) Ovary of *C. enigmdaonta* located between shell muscle and stomach. (**b-c**) Oogenic cells in *C. enigmadonta* at the various stages of development within ovary. (**d**) Ovary of *C. aurora* located between shell muscle and stomach. (**e**) Oogenic cells in *C. aurora* at the various stages of development within ovary. (**f**) Sperm cells in various stages of development in *C. aurora*. MO mature oocyte; O ovary; OO oogonia; PVO previtellogenic oocytes; SC sperm cells under development; SM shell muscle; St stomach; VO vitellogenic oocytes

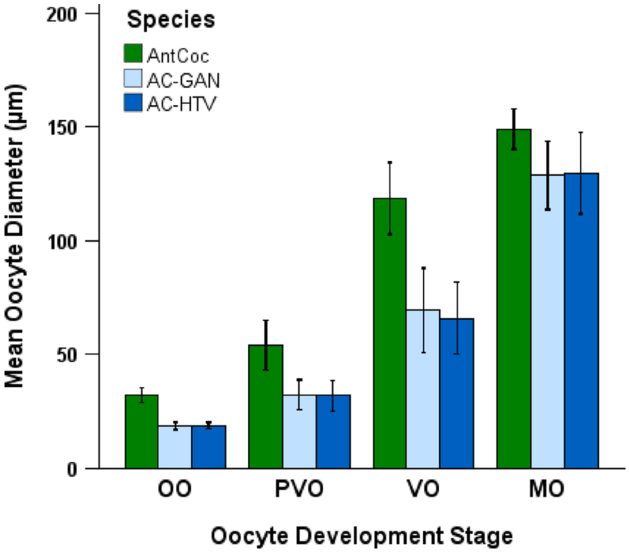

Fig. 6 Mean (± SD) oocyte diameter per oocyte developmental stage for *C. enigmadonta* and *C. aurora*. AntCoc: *C. enigmadonta*, AC-GAN: *C. aurora* from the Ganymede vent and AC-HTV: *C. aurora* from the Hans Tore vent

the same reproductive patterns. Potential variation apparent in the length-frequency histograms could be explained by slight differences in growth and mortality rates, or varying microhabitats and environmental conditions (Matabos and Thiebaut 2010). For both species, the length frequency distributions can be described as 'merging polymodal' distribution. Although, the distributions of both species appear as quasi-unimodal, it is likely the evident distinct peaks in each length-frequency distribution are attributed to numerous recruitments merging into a main size, rather than a singular cohort. In most previous studies to date, discontinuous recruitment has been proposed for hydrothermal vent invertebrates, including the species *Depressigyra globulus* (Kelly and Metaxas 2008), *Protolira valvatoides*, *Pseudorimula midatlantica* (Marticorena et al. 2020), *Riftia pachyptila* (Thiebaut et al. 2002) and *Lepetodrilus elevatus* (Mullineaux et al. 1998). In comparison, continuous recruitment has been suggested for considerably fewer species, including the species *Lepetodrilus fucensis* (Kelly and Metaxas 2008) and *Paralvinella panadorae* (McHugh 1989). Polymodality and evident distinct peaks are indicative of discontinuous recruitment (Kelly and Metaxas 2008; Marticorena et al. 2020), therefore both cocculinid species were deemed to display discontinuous recruitment.

Oogenesis

Histological analysis indicated a similar gametogenic pattern in both study species, with oocytes present in all stages of development, although the oocyte size-ranges and oocyte-size frequency distributions differed. Vitellogenic oocytes were the most abundant in *C. enigmadonta*, whereas previtellogenic oocytes were the most abundant in *C. aurora*. Only three individuals of both *C. engimadonta* and *C. aurora* did not possess all stages of gamete development, which indicates reproduction is asynchronous at population level (Kelly and Metaxas 2007; Matabos and Thiebaut 2010; Marticorena et al. 2020). Furthermore, *C. enigmadonta* exhibited a strong bimodal distribution, with two definitive peaks, which suggests *C. enigmadonta* is iteroparous (Tyler et al. 2008), with developing oocytes separated into two cohorts (Olabarria and Ramirez-Llodra 2004). Bimodal oocyte-size distributions have been reported in other vent gastropod species including *Cyathermia naticoides* and *Rhynochopelta concentrica* (Tyler et al. 2008) and *Nodopelta heminoda*, *Nodopelta subnoda* and *Peltospira operculta* (Matabos and Thiebaut 2010). At both black

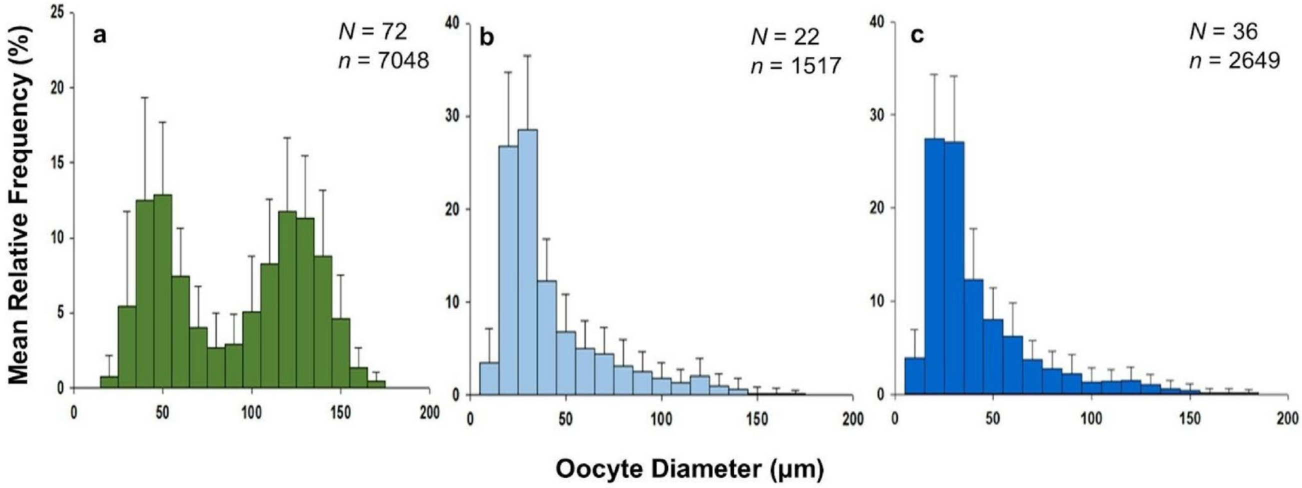

Fig. 7 Mean (± SD) oocyte size-frequency histograms. (**a**) Distribution for pooled individuals of *C. enigmadonta*. Distributions for *C. aurora* individuals from (**b**) Ganymede vent and (**c**) Hans Tore vent. N: number of individuals and n: number of oocytes

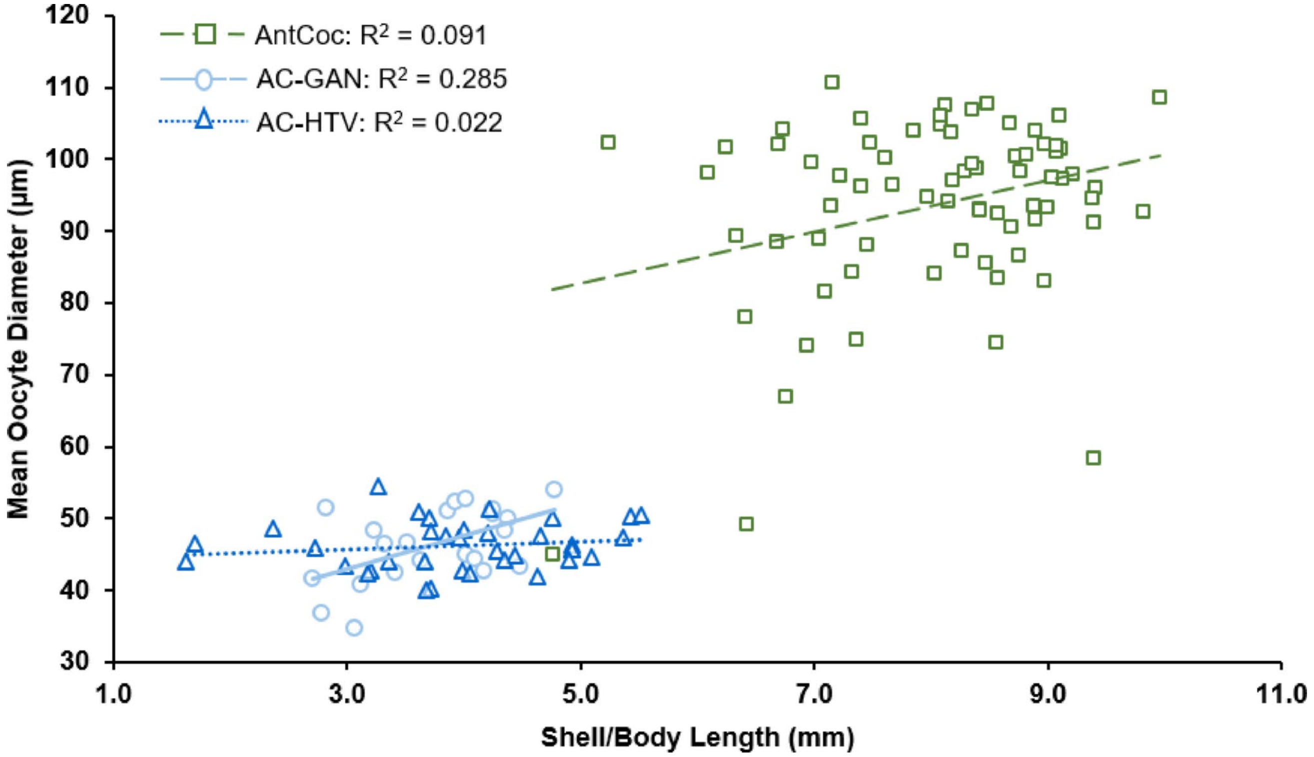

Fig. 8 Relationship between body/shell length and mean oocyte diameter in *C. enigmadonta* and *C. aurora* at the Ganymede and Hans Tore vents. AntCoc: *C. enigmadonta*, AC-GAN: *C. aurora* from the Ganymede vent and AC-HTV: *C. aurora* from the Hans Tore vent

smokers within the AVF, the oocyte-size distributions of *C. aurora* were dominated by previtellogenic oocytes, showing a major peak between 20 and 40 µm and a much smaller peak between 120 and 130 µm corresponding to vitellogenic oocytes. However, this second peak is not significant enough to conclude bimodal distribution for *C. aurora*. Rather, the oocyte-size distribution for *C. aurora* exhibited a positively skewed quasi-unimodal distribution. This distribution is similar to oocyte-size distributions of *Amphissa acutecostata* (Olabarria and Ramirez-Llodra 2004) and of *Lepetodrilus tevnianus* (Bayer et al. 2011). Olabarria and Ramirez-Llodra (2004) suggested a quasi-unimodal oocyte-size distribution was evidence of slow but continuous maturation. Overall, both species have asynchronous reproduction and quasi-continuous gametogenesis because of the presence of all oocyte development stages in all but three individuals. Quasi-continuous gametogenesis would suggest that species have a constant supply of energy, increasing the number of eggs produced. This reproductive pattern is consistent with a continuous energy source produced by chemoautotrophic microorganisms at hydrothermal vents (Tyler et al. 1994).

Reproductive biology

Histological processes are used to determine important information about reproductive patterns and life-history traits; however, these processes can cause tissue shrinkage of up to 20% (Pendlebury 2005) and oocytes can be measured incorrectly if the major axis of the oocyte is not parallel to the plane of the section of the specimen (Copley and Young 2006). Nevertheless, oocyte size is vital in understanding the mode of larval development in deep-sea species (Kelly and Metaxas 2007; Tyler et al. 2008; Marticorena et al. 2020). Planktotrophic larvae are characterised by smaller eggs (< 200 µm), where the small egg size has minimal food reserves and cannot support dispersing larvae, requiring larvae to feed on detritus, phytoplankton and bacteria present in the water column. In comparison, lecithotrophic larvae are associated with larger eggs (> 200 µm), which means that larvae can be sustained by yolks and energy reserves without needing to feed (Tyler 1988; Marticorena et al. 2020). For *C. enigmadonta*, the maximum oocyte size was 185.3 µm and for *C. aurora* it was 183.7 µm, which suggests a planktotrophic development for both species of cocculinid. However, Chen et al. (2022) utilised a scanning electron microscope to investigate the protoconch and teleconch structures of *C. aurora*. The shell size and structure was indicative of a gastropod which exhibits lecithotrophic larval development. Additionally, in all other cocculinid species examined to date, the protoconch structure suggests they are lecithotrophic (Marshall 1985; Haszprunar 1988). Unfortunately, the shells *C. enigmadonta* individuals in this study and Chen and Linse (2020) were highly degraded, thus the larvae development could not be inferred using a scanning electron microscope. When considering oocyte shrinkage and phylogenetical constraints, it is likely *C. enigmadonta* exhibits lecithotrophic larval development.

Early maturation in vent species is seen as an advantageous life-history trait which is indicative of opportunistic species (Bridges et al. 1994). The minimum size of reproductive maturity was defined as the size at first development of mature oocytes. The minimum size of reproductive maturity was 5.23 mm in *C. enigmadonta.* In *C. aurora*, the minimum size of maturity was 2.70 mm at the Ganymede vent, and 1.62 mm at the Hans Tore vent. Reproductive maturity occurs at around half of the maximum size for *C. enigmadonta* (52.7%) and a third of maximum size for *C. aurora* (29.4%). Young et al. (2013) found that the size of development of mature gametes was similar in *Cocculina rathbuni* which was 37.5%. Conversely, Kelly and Metaxas (2007) reported that the species *Lepetodrilus fucensis* possessed mature oocytes at ~16.7% of their maximum shell length and the species *Lepetodrilus elevatus* possessed mature oocytes at ~33.3% of their maximum shell length. In comparison to these species, *C. enigmadonta* had a relatively high minimum size for mature gamete development. *Cocculina enigmadonta* and *C. aurora* had a similar maximum oocyte diameter, however the size of oocyte development, mean oocyte diameter, the size of vitellogenesis, and mean mature oocyte diameter all differed. The mean mature oocyte diameter was 149.0 µm for *C. enigmadonta* and 129.0 µm for *C. aurora*. These differences are likely related to the difference in the overall size of the species, with *C. enigmadonta* being much larger than *C. aurora.*

Fecundity

Instantaneous fecundity was statistically significantly greater in *C. enigmadonta*, than the *C. aurora* indicating there is considerable inter-species variation. Direct comparisons between the size of each species is difficult as body length was measured for *C. enigmadonta*, and shell length was measured for *C. aurora* individuals. Nevertheless, the mean body length of reproductively mature *C. enigmadonta* individuals (8.08 mm) was more than double that of *C. aurora* (3.91 mm). The difference in fecundity is likely a function of the significant size disparity between *C. enigmadonta* and *C. aurora*. Individuals of the family Cocculinidae are typically less than 1 cm in size (Chen and Linse 2020), thus *C. enigmadonta* is a relatively 'big' species of cocculinid. Young et al. (2013) investigated recruitment and fecundity in two other cocculinid species namely, *Cocculina rathbuni* and *Cocculina emsoni*. They found a shell length of 1.5–4.0 mm for both species. These sizes were similar to *C. aurora* in the present study (1.62–5.51 mm). Young et al. (2013) found that instantaneous fecundity was limited to 40 oocytes in *C. rathbuni* and *C. emsoni*, due to their 'diminutive size'. The maximum instantaneous fecundity recorded for *C. aurora* was 12 which is much lower than *C. rathbuni* and *C. emsoni.* In comparison, the maximum instantaneous fecundity for *C. enigmadonta* was 39. Nonetheless, opportunistic life-history traits are possessed for cocculinid limpets, including small body sizes, and high growth rates (Young et al. 2013), but low fecundity and relatively large size at maturity are not usually exhibited by opportunistic species. Both species were found to be abundant at their respective sampling locations, however, which suggests that their apparent low fecundity does not limit survival and recruitment.

62% of hydrothermal vent molluscs have been listed as threatened by the International Union for Conservation of Nature (IUCN) (Thomas et al. 2021). Climate change (Sweetman et al. 2017; Ross et al. 2020) and pollution (Barrett et al. 2020; Krause et al. 2020) continues to affect the marine environment, whilst the impacts of mining massive sulphides on hydrothermal vents is the centre of discussions for the development of regulations in this field (Miller et al. 2018; Niner et al. 2018). Investigating the reproductive biology of deep-sea vent molluscs is vital to understand the resilience and recovery potential of hydrothermal vent species and communities in response to anthropogenic impacts (Hilário et al. 2015; Van Dover et al. 2018). Both *C. enigmadonta* and *C. aurora* in this study were sampled from hydrothermal vents, and both species display advantageous reproductive adaptations and life-history traits including asynchronous reproduction, quasi-continuous gametogenesis, and small body sizes. Conversely, they exhibit low fecundities and relatively large size at maturity in comparison to other hydrothermal vent gastropods (Kelly and Metaxas 2007; Young et al. 2013), which would potentially hinder recovery and resilience of both cocculinid species to natural and anthropogenic disturbance. Furthermore, both species were abundant at their respective sampling locations, therefore *C. enigmadonta* and *C. aurora* gene flow and connectivity amongst vent sites within a region need to be better understood in order to assess impacts and recovery potential from exploitation activities to develop robust management plans (Hilário et al. 2015).

Conclusion

This study describes the reproductive biology of the first cocculinid species sampled from hydrothermal vents, *Cocculina enigmadonta* from vents in the Southern Ocean and *Cocculina aurora* collected from vents under permanent ice cover in the Arctic. Both species have similar patterns including quasi-continuous gametogenesis, asynchronous reproduction, and discontinuous reproductive patterns with low fecundities and early maturation. However, they differ in mean oocyte diameter, size of vitellogenesis and gametogenic size patterns. Where this study compared the reproductive biology of cocculinid species from hydrothermal vents, future work should focus on comparing the reproductive biology of cocculinid species associated with natural falls and hydrothermal vents, as well as gene flow amongst populations. Furthermore, it is important to determine the small-scale environmental variation between black smokers to elucidate observed variations in certain reproductive traits of *C. aurora* from different black smokers in the AVF. A full understanding of life history traits in vent species is essential to mitigate the potential for habitat destruction associated with mineral exploitation in the deep sea.

Supplementary Information The online version contains supplementary material available at https://doi.org/10.1007/s00227-025-04648-x.

Acknowledgements The authors would like to thank the captain and crew of the RRS *James Cook* on JC42 expedition and RV *Kronprins Haakon* on the HACON21 expedition for their support with scientific work at sea. We also thank the pilots and teams of the ROV *Isis* and *Aurora* for their sampling efforts. We are very grateful to Gerhard Bohrmann, Alex. D Rogers and Stefan Bünz as principal/chief scientists on their respective expeditions. Chong Chen is acknowledged for his help in initial identification of *C. enigmadonta* samples, Adam Reed is acknowledged for his help with histological processing and oocyte analysis techniques and Tammy Horton is acknowledged for her teachings in relation to microscope usage and dissection.

Author contributions All authors contributed to the design of the study. Data collection was performed by Maria Baker, Jon Copley, Paul Tyler, Ana Hilario and Eva Ramirez-Llodra. Data analysis was performed by Christopher MacNeil. The first draft was completed by Christopher MacNeil, and all authors provided comments on changes of previous versions of the manuscript. All authors read and approved the final manuscript.

Funding The JC42 expedition was funded by the UK NERC Consortium Grant NE/DO1249X/1 (Paul Tyler Principal Investigator). The shiptime of the HACON21 expedition was funded by the Norwegian Research Council through a FRINATEK grant (274330) and UiT. Christopher MacNeil thanks the University of Southampton, UK for the funding support provided for the associated Master of Research project. Ana Hilário was supported by funds from FCT/MCTES granted to CESAM (UIDP/50017/2020 + UIDB/50017/2020 + LA/P/0094/2020).

Data Availability Data has been provided as Supplementary Material.

Declarations

Conflict of interest The authors have no conflicts of interest to declare that are relevant to the content of this article.

Ethical approval All applicable international, national, and/or institutional guidelines for sampling were followed in the current study.

References

Amon DJ, Glover AG, Wiklund H, Marsh L, Linse K, Rogers AD, Copley JT (2013) The discovery of a natural Whale fall in the Antarctic deep sea. Deep-Sea Res II: Top Stud Oceanogr 92:87–96. https://doi.org/10.1016/j.dsr2.2013.01.028

Barrett J, Chase Z, Zhang J, Holl MMB, Willis K, Williams A, Hardesty BD, Wilcox C (2020) Microplastic pollution in deep-sea sediments from the great Australian bight. Front Mar Sci 7:576170. https://doi.org/10.3389/fmars.2020.576170

Bayer SR, Mullineaux LS, Waller RG, Solow AR (2011) Reproductive traits of pioneer gastropod species colonizing deep-sea hydrothermal vents after an eruption. Mar Biol 158:181–192. https://doi.org/10.1007/s00227-010-1550-1

Bhattacharya CG (1967) A simple method of resolution of distribution into Gaussian components. Biometrics 23(1):115–135. https://doi.org/10.2307/2528285

Boetius A (2015) The expedition PS86 of the research vessel POLARSTERN to the Arctic ocean in 2014. Rep Polar Mar Res 685:1–133. https://doi.org/10.2312/BzPM_0685_2015

Bouchet P, Rocroi J, Hausdorf B, Kaim A, Kano Y, Nützel A, Parkhaev P, Schrödl M, Stron EE (2017) Revised classification, nomenclator and typification of gastropod and monoplacophoran families. Malacologia 61(1–2):1–526. https://doi.org/10.4002/040.061.0201

Bridges TS, Levin LA, Cabrera D, Plaia G (1994) Effects of sediment amended with sewage, algae, or hydrocarbons on growth and reproduction in two opportunistic polychaetes. J Exp Mar Biol Ecol 177(1):99–119. https://doi.org/10.1016/0022-0981(94)90146-5

Bünz S, Ramirez-Llodra E, Victorero L, Ferre B, Panieri G, Dessandier P, Kalenitchenko D, Sert F, Rapp HT, Steen I, Reeves E, Meckel EM, Mall A, Ribeiro P, Dahle H, Vulcano F, Kutti T, German C, Hand K, Klesh A, Purser A, Hoge U, Hilario A, Ramalho S, Jukuba M, Bowen A, Suman S, Gomez-Ibanez D, Judge C, Curran M, Naklicki, Vågenes P, Lumar L, Drake N (2021) RV *Kronprins Håkon* (cruise no. 2021711) Longyearbyen-Longyearbyen 28.09.2021-21.10.2021. Tromsø: UiT The Arctic University of Norway

Chen C, Linse K (2020) From wood to vent: first cocculinid limpet associated with hydrothermal activity discovered in the Weddell sea. Antarct Sci 32(5):354–366. https://doi.org/10.1017/S095410202000022X

Chen C, Hilario A, Rodrigues CF, Ramirez-Llodra E (2022) Integrative taxonomy of a new cocculinid limpet dominating the Aurora vent field in the central Arctic ocean. Royal Soc Open Sci 9:220885. https://doi.org/10.1098/rsos.220885

Copley JTP, Young CM (2006) Seasonality and zonation in the reproductive biology and population structure of the shrimp *Alvinocaris stactophila* (Caridea: Alvinocarididae) at a Louisiana slope cold seep. MEPS 315:199–209. https://doi.org/10.3354/meps315199

Edmonds HN, Michael PJ, Baker ET, Connelly DP, Snow JE, Langmuir CH, Dick HJB, Mühe R, German RC, Graham DW (2003) Discovery of abundant hydrothermal venting on the ultraslow-spreading Gakkel ridge in the Arctic ocean. Nature 421:252–256. https://doi.org/10.1038/nature01351

German RC, Reeves EP, Türke A, Diehl A, Albers E, Bach W, Purser A, Ramalho SP, Suman S, Mertens C, Walter M, Ramirez-Llodra E, Schlindwein V, Bünz S, Boetius A (2022) Volcanically hosted venting with indications of ultramafic influence at Aurora hydrothermal field on Gakkel Ridge. Nat Commun. https://doi.org/10.1038/s41467-022-34014-0

Gustafson RG, Littlewood DTJ, Lutz RA (1991) Gastropod egg capsules and their contents from deep-sea hydrothermal vent environments. Biol Bull 180:34–55

Haszprunar G (1988) Comparative anatomy of cocculiniform gastropods and its bearing on archaeogastropod systematics. Malacol Rev (Suppl 4): 64–84

Hilário A, Metaxas A, Gaudron SM, Howell KL, Mercier A, Mestre NC, Ross RE, Thrunherr AM, Young C (2015) Estimating dispersal distance in the deep Sea: challenges and applications to marine reserves. Front Mar Sci. 2:6. https://doi.org/10.3389/fmars.2015.00006

Hoffman L, Gofas S, Freiwald A (2020) Ten new species in *Papuliscala* de Boury, 1911 (Gastropoda, Epitoniidae) from the South Azorean seamount chain. Iberus 38(1):29–53

Jaeckle W (1995) Variation in the size, energy content, and biochemical composition of invertebrate eggs: correlates to the mode of larval development. In: McEdward LR (ed) Ecol of Mar inver Larv, L. CRC, Boca Raton, FL, pp 49–77

Kelly NE, Metaxas A (2007) Influence of habitat on the reproductive biology of the deep-sea hydrothermal vent limpet *Lepetodrilus fucensis* (Vetigastropoda: Mollusca) from the Northeast Pacific. Mar Biol 151:649–662. https://doi.org/10.1007/s00227-006-0505-z

Kelly NE, Metaxas A (2008) Population structure of two deep-sea hydrothermal vent gastropods from the Juan de fuca ridge, NE Pacific. Mar Biol 153:457–471. https://doi.org/10.1007/s00227-007-0828-4

Krause S, Molari M, Gorb EV, Kossel E, Haeckel M (2020) Persistence of plastic debris and its colonization by bacterial communities after two decades on the abyssal seafloor. Sci Rep 10:9484. https://doi.org/10.1038/s41598-020-66361-7

Lau SCY, Grange LJ, Peck LS, Reed AJ (2018) The reproductive ecology of the Antarctic bivalve *Aequiyoldia eightsii* (Protobranchia: Sareptidae) follows neither Antarctic nor taxonomic patterns. Polar Biol 41:1693–1706. https://doi.org/10.1007/s00300-018-2309-2

Levin LA, Bridges TS (1995) Pattern and diversity in reproduction and development. In: McEdward LR (ed) Ecol Mar inver Larv. CRC, Boca Raton, Florida, pp 1–48

Linse K, Copley JT, Connelly DP, Larter RD, Pearce DA, Polunin NVC, Rogers AD, Chen C, Clarke A, Glover AG, Graham AGC, Huvenne VAI, Marsh L, Reid WDK, Roterman CN, Sweeting CJ, Zwirglmaier K, Tyler PA (2019) Fauna of the Kemp caldera and its upper bathyal hydrothermal vents (South sandwich Arc, Antarctica). Royal Soc Open Sci 6:191501. https://doi.org/10.1098/rsos.191501

Lutz RA (1988) Dispersal of organisms at deep-sea hydrothermal vents: a review. Oceanologica Acta. https://archimer.ifremer.fr/doc/00267/37831/. Accessed from 12 August 2022

Lutz RA, Jablonski D, Turner RD (1984) Larval development and dispersal at deep-sea hydrothermal vents. Science 226(4681):1451–1454. https://doi.org/10.1126/science.226.4681.1451

Macdonald P (2018) Mixdist: finite mixture distribution models

Marshall BA (1985) Recent and tertiary Cocculinidae and Pseudococculinidae (Mollusca: Gastropoda) from new Zealand and new South Wales. N Z J Zool 12(4):505–546. https://doi.org/10.1080/03014223.1985.10428301

Marticorena J, Matabos M, Sarrazin J, Ramirez-Llodra E (2020) Contrasting reproductive biology of two hydrothermal gastropods from the Mid-Atlantic Ridge: implications for resilience of vent communities. Mar Biol 167:109. https://doi.org/10.1007/s00227-020-03721-x

Matabos M, Thiebaut E (2010) Reproductive biology of three hydrothermal vent peltospirid gastropods (*Nodopelta heminoda*, *N. subnoda* and *Peltospira operculate*) associated with pompeii worms on the East Pacific rise. J Molluscan Stud 76(3):257–266. https://doi.org/10.1093/mollus/eyq008

McHugh D (1989) Population structure and reproductive biology of two sympatric hydrothermal vent polychaetes, *Paralvinella Pandorae* and *P. palmiformis*. Mar Biol 103:95–106. https://doi.org/10.1007/BF00391068

McLean JH (1992) Cocculiniform limpets (Cocculinidae and Pyropeltidae) living on Whale bone in the deep sea off California. J Moll Stud 58(4):401–414. https://doi.org/10.1093/mollus/58.4.401

Michael PJ, Langmuir CH, Dick HJB, Snow JE, Goldstein SL, Graham DW, Lehnert K, Kurras G, Jokat W, Mühe R, Edmonds HN (2003) Magmatic and amagmatic seafloor generation at the ultraslow-spreading Gakkel ridge, Arctic ocean. Nature 423:956–961. https://doi.org/10.1038/nature01704

Miller KA, Thompson KF, Johnston P, Santillo D (2018) An overview of seabed mining including the current state of development, environmental impacts, and knowledge gaps. Front Mar Sci 4:418. https://doi.org/10.3389/fmars.2017.00418

Mullineaux LS, Mills SW, Goldman E (1998) Recruitment variation during a pilot colonization study of hydrothermal vents (9°50’N, East Pacific Rise). Deep-Sea Res II 45(1–3):441–464. https://doi.org/10.1016/S0967-0645(97)00045-3

Niner HJ, Ardron JA, Escobar EG, Gianni M, Jaeckel A, Jones DOB, Levin LA, Smith CR, Thiele T, Turner PJ, Van Dover CL, Watling L, Gjerde KM (2018) Deep-sea mining with no net loss of biodiversity– an impossible aim. Front Mar Sci 5:53. https://doi.org/10.3389/fmars.2018.00053

Nützel A, Lehnert O, Frýda J (2006) Origin of planktotrophy– evidence from early molluscs. Evol Dev 8(4):325–330. https://doi.org/10.1111/j.1525-142X.2006.00105.x

Olabarria C, Ramirez-Llodra E (2004) Reproductive strategies of two deep-sea gastropod species from the Porcupine seabight (Northeast Atlantic). Mar Biol 145:541–549. https://doi.org/10.1007/s00227-004-1333-7

Paul D, Caddy JF (1985) A modification of Bhattacharya’s method for the analysis of mixtures of normal distributions. FAO Fisheries Circular

Pendlebury SJD (2005) Ecology of hydrothermal vent gastropods (*Lepetodrilus elevatus*, *Rhyncopelta concentrica*, *Cyanthermia naticoides*). Dissertation, University of Southampton

Ramirez-Llodra E (2002) Fecundity and life-history strategies in marine invertebrates. Adv Mar Biol 43:87–170. https://doi.org/10.1016/S0065-2881(02)43004-0

Ramirez-Llodra E, Brandt A, Danovaro R, De Mol D, Escobar E, German CR, Levin LA, Martinez Arbizu P, Menot L, Buhl-Mortensen P, Narayanaswamy BE, Smith CR, Tittensor DP, Tyler PA, Vanreusel A, Vecchione M (2010) Deep, diverse and definitely different: unique attributes of the world's largest ecosystem. Biogeosciences 7:2851–2899. https://doi.org/10.5194/bg-7-2851-2010

Ramirez-Llodra E, Argentino C, Baker M, Boetius A, Costa C, Dahle H, Denny EM, Dessandier P, Eilertsen MH, Ferre B, German CR, Hand K, Hilário A, Hislp L, Jamieson JW, Kalnitchenko D, Mall A, Panieri G, Purser A, Ramalho SP, Reeves EP, Rolley L, Pereira SI, Ribeiro PA, Sert MF, Steen IH, Stetzler M, Stokke R, Victorero L, Vulcano F, Vågenes S, Waghorn KA, Buenz S (2022) Hot vents beneath an icy ocean: The Aurora vent field, Gakkel Ridge, revealed. J Oceanogr. https://doi.org/10.5670/oceanog.2023.103

Rokop FJ (1977) Seasonal reproduction of the brachiopod *Frieleia halli* and the scaphopod *Cadulus californicus* at bathyal depths in the deep sea. Mar Biol 43:237–246. https://doi.org/10.1007/BF00402316

Ross T, Du Preez C, Lanson D (2020) Rapid deep ocean deoxygenation and acidification threaten life on Northeast Pacific seamounts. Glob Chang Biol 26(11):6424–6444. https://doi.org/10.1111/gcb.15307

Roterman CN, Copley JT, Linse KT, Tyler PA, Rogers AD (2016) Connectivity in the cold: the comparative population genetics of vent-endemic fauna in the Scotia Sea, Southern ocean. Mol Ecol 25(5):1073–1088. https://doi.org/10.1111/mec.13541

Schneider CA, Rasband WS, Eliceiri KW (2012) NIH image to imageJ: 25 years of image analysis. Nat Methods 9:671e675. https://doi.org/10.1038/nmeth.2089

Sweetman AK, Thurber AR, Smith CR, Levin LA, Mora C, Wei C, Gooday AJ, Jones DOB, Rex M, Yasuhara M, Ingels J, Ruhl HA, Frieder CA, Danovaro R, Würzberg L, Baco A, Grupe BM, Pasulka A, Meyer KS, Dunlop KM, Henry L, Roberts JM (2017) Major impacts of climate change on deep-sea benthic ecosystems. Elem Sci Anth 5:4. https://doi.org/10.1525/elementa.203

Thiebaut E, Huther X, Shillito B, Jollivet D, Gaill F (2002) Spatial and Temporal variations of recruitment in the tube worm *Riftia pachyptila* on the East Pacific rise (9°50'N and 13°N). Mar Ecol Prog Ser 234:147–157. https://doi.org/10.3354/meps234147

Thomas EA, Molloy A, Hanson NB, Böhm M, Seddon M, Sigwart JD (2021) A global red list for hydrothermal vent molluscs. Front Mar Sci 8:713022. https://doi.org/10.3389/fmars.2021.713022

Tyler PA (1988) Seasonality in the deep sea. Oceanogr Mar Biol Annu Rev 26:227–258

Tyler PA, Young CM (1999) Reproduction and dispersal at vents and cold seeps. J Mar Biol Ass U K 79:193–208. https://doi.org/10.1017/S0025315499000235

Tyler PA, Campos-Creasey LS, Giles LA (1994) Environmental control of quasi-continuous and seasonal reproduction in deep-sea benthic invertebrates. In: Young CM, Eckelbarger KJ (eds) Reproduction, larval biology, and recruitment of the deep-sea benthos, 1st edn. Columbia University, New York, pp 158–178

Tyler PA, Pendlebury S, Mills SW, Mullineaux L, Eckelbarger KJ, Baker M, Young CM (2008) Reproduction of gastropods from vents on the East Pacific rise and the Mid-Atlantic ridge. J Shellfish Res 27(1):107–118. https://doi.org/10.2983/0730-8000(2008)27[107:ROGFVO]2.0.CO;2

Van Dover CL (2000) The ecology of deep-sea hydrothermal vents. Princeton University Press, Princeton. https://doi.org/10.1515/9780691239477

Van Dover CL, Arnaud-Haond S, Gianni M, Helmreich S, Huber JA, Jaeckel AL, Metaxas A, Pendleton LH, Petersen S, Ramirez-Llodra E, Steinberg PE, Tunnicliffe V, Yamamoto H (2018) Scientific rationale and international obligations for protection of active hydrothermal vent ecosystems from deep-sea mining. Mar Policy 90:20–28. https://doi.org/10.1016/j.marpol.2018.01.020

Vrijenhoek RC (1997) Gene flow and genetic diversity in naturally fragmented metapopulations of deep-sea hydrothermal vent animals. J Hered 88(4):285–293. https://doi.org/10.1093/oxfordjournals.jhered.a023106

Yahagi T, Thaler AD, Van Dover CL, Kano Y (2020) Population connectivity of the hydrothermal-vent limpet *Shinkaliepas tollmanni* in the Southwest Pacific (Gastropoda: neritimorpha: Phenacolepadidae). PLoS ONE 15(9):e0239784. https://doi.org/10.1371/journal.pone.0239784

Young CM, Emson RH, Rice ME, Tyler PA (2013) A Paradoxical mismatch of fecundity and recruitment in deep-sea opportunists: cocculinid and pseudococculinid limpets colonizing vascular plant remains on the Bahamian slope. Deep-Sea Res II: Top Stud Oceanogr 92:36–45. https://doi.org/10.1016/j.dsr2.2013.01.027

Zhang S, Zhang S (2018) *Cocculina delphinicula* Sp. nov., a new cocculinid Sp.cies from Whale bone in the East China sea (Gastropoda: Cocculiniformia). Zootaxa 4455:189–195. https://doi.org/10.11646/zootaxa.4455.1.9